Sedimentary development of a continuous Middle Devonian to Mississippian section from the fore-reef fringe of the Brilon Reef Complex (Rheinisches Schiefergebirge, Germany)

Damien Pas, Anne-Christine Da Silva, Pierre Cornet, Pierre Bultynck, Peter Königshof & Frédéric Boulvain

Facies
International Journal of Paleontology, Sedimentology and Geology

ISSN 0172-9179
Volume 59
Number 4

Facies (2013) 59:969-990
DOI 10.1007/s10347-012-0351-z

Springer

Facies (2013) 59:969–990
DOI 10.1007/s10347-012-0351-z

ORIGINAL ARTICLE

Sedimentary development of a continuous Middle Devonian to Mississippian section from the fore-reef fringe of the Brilon Reef Complex (Rheinisches Schiefergebirge, Germany)

Damien Pas · Anne-Christine Da Silva · Pierre Cornet · Pierre Bultynck · Peter Königshof · Frédéric Boulvain

Received: 4 June 2012 / Accepted: 19 November 2012 / Published online: 22 December 2012

Abstract The Brilon-reef complex is one of the biggest Devonian carbonate buildups ($\sim$80 km^2) of the Rheinisches Schiefergebirge. The Burgberg section is located in the southeastern fore-reef area of the Brilon Reef Complex and exposes a succession of strata (117 m thick), which extends from the Middle Givetian (middle *varcus* conodont Zone) to the Viséan (*bilineatus* conodont Zone). Field and microfacies observations led to the definition of nine microfacies that are integrated into a sedimentary model divided into off-reef, intermediate fore-reef, and proximal fore-reef sedimentary domains (SD). The off-reef domain (SD1) is the most distal setting observed and is characterized by fine-grained sediments, dominated by pelagic biota and the local occurrence of gravity-flow deposits. The intermediate fore-reef (SD2) is characterized by a mixture of biota and sediments coming from both deeper-water and shallow-water sources and is influenced by storm and gravity-flow currents. In this domain, *Renalcis* mound-like structures developed locally. Finally, the proximal fore-reef (SD3) corresponds to the most proximal setting that is strongly influenced by gravity-flow currents derived from the Brilon Reef Complex. The temporal evolution of microfacies in the fore-reef setting of the Burgberg section show five main paleoenvironmental trends influenced by the onset, general development, and demise/drowning of the Brilon Reef Complex. Fore-reef to off-reef lithologies and their temporal changes are from the base to the top of the section: (U1)—fine-grained sediments with large reef debris, corresponding to the initial development of the reef building upon submarine volcaniclastic deposits during the Middle Givetian (middle *varcus* Zone) and first export of reef debris in the fore-reef setting; (U2)—high increase of reef-derived material in the fore-reef area, corresponding to a significant progradation of the reef from the Middle Givetian to the Early Frasnian (maximum extension of the Brilon Reef Complex to the south, *disparilis* to the *falsiovalis* conodont biozones); (U3)—progressive decrease of shallow-water derived material and increase of fine-grained sediments and deep-water biota into the fore-reef setting, corresponding to the stepwise withdrawal of the reef influence; from the Middle to the Late Frasnian (*jamieae* conodont Zone); (U4)—development of a submarine rise characterized by nodular and cephalopod-bearing limestones extending from the Late Frasnian to the Late Famennian corresponding to the demise and drowning of the Brilon Reef Complex as a result of the Late Frasnian Kellwasser events (upper *rhenana* and *triangularis* conodont biozones); (U5)—significant deepening of the Burgberg area starting in the Late Famennian, directly followed by an aggrading trend marked by pelagic shales overlying the nodular limestone deposits.

Keywords Microfacies · Brilon fore-reef · Rheinisches Schiefergebirge · Mid-Late Devonian · Carboniferous · Sedimentology · Kellwasser events

D. Pas (✉) · A.-C. Da Silva · P. Cornet · F. Boulvain
Sedimentary Petrology, B20, University of Liège (ULg), Sart-Tilman, 4000 Liège, Belgium
e-mail: dpas@ulg.ac.be

P. Bultynck
Department of Paleontology, Royal Belgian Institute of Natural Sciences, rue Vautier 29, 1000 Brussels, Belgium

P. Königshof
Senckenberg, Research Institute and Natural History Museum Frankfurt, Senckenberganlage 25, 60325 Frankfurt, Germany

Introduction

During Middle Devonian time, the Brilon Reef Complex, western Germany, belonged to a large carbonate platform belt developed at the southern margin of the Old Red Continent. This reef complex is considered to be one of the largest Middle Devonian carbonate buildups (~80 km^2) identified within the eastern Rheinisches Schiefergebirge (RS). Among the various Middle Devonian reef complexes recognized throughout the world (Copper 2002), the Brilon Reef Complex is one of the first studied and most investigated. The mapping, stratigraphic, and facies studies of the 1930s and 1960s provided a first summary on the dimension of the reef complex and an overview on the main lithologies and their distribution pattern in the area (Paeckelmann 1936; Jux 1960; Bär 1968). Aiming to characterize the Devonian reefs of Central Europe, Krebs (1967, 1971, 1974) interpreted the Brilon reef as an "isolated carbonate complex (atoll) at the outer shelf margin." Using new data from the federal drilling project, Brinckmann (1981) identified two steps of reef growth: an early phase at the northern margin of the complex, beginning in the Middle Devonian (possibly as early as Eifelian), and a later phase at the southern margin beginning in the Late Givetian. However, the reef growth might have started earlier in the southern margin, as Malmsheimer et al. (1990) identified the first reef-related debris during the lower *varcus* Zone (early Givetian).

Reef growth at the northern and southern margin during Late Givetian and Early Frasnian resulted in the formation of an atoll-like reef (Brinckmann 1981). Based on drill core from the south of the Brilon Reef Complex, Machel (1990) developed a model for the Middle Devonian and Early Frasnian facies including back-reef, reef-core, and fore-reef setting. Using this model, Machel (1990) recognized three main stages of carbonate sedimentation in the Brilon Reef Complex: (1) Initiation of carbonate sedimentation starting with the final phase of Middle Devonian volcanism, (2) major accumulation of "reefal sediment", and (3) deposition of sediment in which reef influence is not clearly defined. Conodont biostratigraphy indicates that carbonate sedimentation commenced in the Late Givetian and lasted until at least the beginning of the Frasnian but the Givetian-Frasnian boundary was not clearly identified (Machel 1990). Machel (1990) and Städter and Koch (1987) recognized that through the Upper Givetian, the reef-core shifted gradually towards the basin located in the southeast. In the same period, Stritzke (1990) performed a general facies study of the southeastern margin of the Brilon Reef Complex on the basis of 15 sections (including the Burgberg section). This study resulted in the definition of three main facies corresponding to reef-core, fore- and off-reef setting, and their evolution from the Middle Givetian to the Upper Famennian (middle v*arcus* to lower *bisphatodus* zones).

In summary, the Brilon Reef Complex was the subject of various studies providing a good overview on the major facies belts and their general evolution through time. However, a comprehensive study integrating the entire development of the reef (onset, expansion, and drowning) built on a detailed facies description of a long and continuous interval was still lacking. In this paper, we document a detailed sedimentological study of the continuous Middle Givetian to Viséan interval (~40 Ma) recorded in the Burgberg section in order to provide a detailed sedimentological model covering the entire sequence of facies in the southeastern area of the Brilon Reef Complex. We combined paleontological and sedimentological datasets from the literature and new geochemical data ($\delta^{13}C$ analysis around the Frasnian-Famennian boundary) in order to gain a better understanding of the depositional and environmental changes in a fore-reef setting within the Rheinisches Schiefergebirge. Moreover, the good biostratigraphic control of most of the succession offers the first opportunity to provide a well-constrained timing of the onset, main development, and demise/drowning of the reefal structure in its southeastern part and to improve our knowledge of global changes over a long time scale. This outstanding succession in a fore-reef setting is also an opportunity to evaluate the potential of a single section in the recognition of major paleoenvironmental changes occurring in shallow-water reefal habitats.

Location and geological background

The Rhenohercynian Massif (RM) is composed of Paleozoic (Ordovician to Carboniferous) sedimentary and volcanic rocks that were accumulated in the southern part of the Old Red Continent. The RM extends east to west from the Ardennes area in Belgium to the Rheinisches Schiefergebirge and the Harz Mountains in Germany. The rocks of the RM were deformed and folded during the Variscan orogeny; deformation and very low to low-grade metamorphism prograded from the SE to NW during the Late Carboniferous Period (e.g., Ahrendt et al. 1983). During the Middle Devonian, the Burgberg section was located on the southern margin of the Old Red Continent within the Rhenohercynian Basin (Fig. 1), close to the Brilon Reef Complex. In the late Early and Middle Devonian, eustatic sea level rise, leading to a shoreline shifts to the north (e.g., Johnson 1970; Johnson et al. 1985; House 1985), deeply changed the sedimentary setting of the southern margin of the Old Red Continent. The onset of these significant sea-level changes is marked by the change from siliciclastic, deltaic shallow-marine environments ("Rhenish" facies) in

the Lower Devonian, to an open-marine argillaceous shale and pure limestone-dominated facies ("Hercynian" facies) in the Middle Devonian (Erben 1962). This transgression resulted in the development of Middle Devonian large-scale reef structures in the RS, such as the Brilon Reef Complex.

During the Middle Devonian, extensional tectonics in the southern and eastern part of the RS lead to submarine volcanism (summary and further references in Nesbor 2004; Kroner et al. 2007; Königshof et al. 2010; Salamon and Königshof 2010). This volcanism produced submarine rises that enabled reef growth in a basinal facies setting, and the southern fringe area of the Brilon Reef Complex is thought to have developed simultaneous to the placement of these volcanic rocks ("Hauptgrünsteinzug") in a basinal setting (Sunkel 1990). At the southeastern margin of Brilon, accumulation of reef debris started in the Middle Givetian (lower *varcus* Zone) (Malmsheimer et al. 1990), while in the northern part it started in the Lower Devonian (possibly as early as Eifelian) (Brinckmann 1981). Flourishing reef growth at the northern and southern margin from the Late Givetian to the Early Frasnian led to the establishment of an atoll-like reef (Brinckmann 1981). During the Upper Devonian, the drowning of the Brilon Reef Complex is confirmed by Upper Devonian and Lower Carboniferous condensed cephalopod limestones overlying the Brilon Reef Complex (Malmsheimer et al. 1990). In terms of regional geology, the Burgberg section belongs to the northern flank of the Messinghausen anticline (Fig. 2), southeast of the Brilon anticline. In the eastern RS, the Middle Devonian reefal limestone is referred to as "Massenkalk" (von Dechen 1858). According to Krebs (1967, 1974), the "Massenkalk" can be divided into three lithologic units: (1) an initial biostromal "bank-type Massenkalk" ("Schwelm" facies of Paeckelmann 1922); (2) a subsequent biohermal "reef-type Massenkalk" ("Dorp" facies of Krebs 1967); (3) a "cap-type Massenkalk" ("Iberg" facies of Krebs 1967). The time-equivalent of the "Massenkalk" in the off-reef and back-reef setting is called the "Flinz" facies. A summary of the lithostratigraphic subdivision of the Brilon area is given in Fig. 3.

Materials and methods

A detailed bed-by-bed description of the Burgberg sections (Figs. 4, 5) and sampling was performed, with average sampling rate of one sample per 25 cm (a total of 340 samples for thin-sections). The textural classification used to characterize the microfacies follows Dunham (1962) and Embry and Klovan (1972). Estimation of sorting is based on the visual charts of Pettijohn et al. (1972), while visual percentage estimation is based on the comparison charts of Bacelle and Bosellini (1965). Thin-sections were stained using Dickson solution (1965) to differentiate calcite, dolomite, ferroan calcite, and ferroan dolomite. Fourteen samples (±400 g) from pelagic facies were taken for conodont investigation. Conodonts are common, most samples containing 25–50 specimens/kg.

Analyses of $\delta^{13}C_{carb}$ were done using bulk mudstone-wackestone samples. Powdered samples reacted with phosphoric acid in an online carbonate preparation (Kiel III

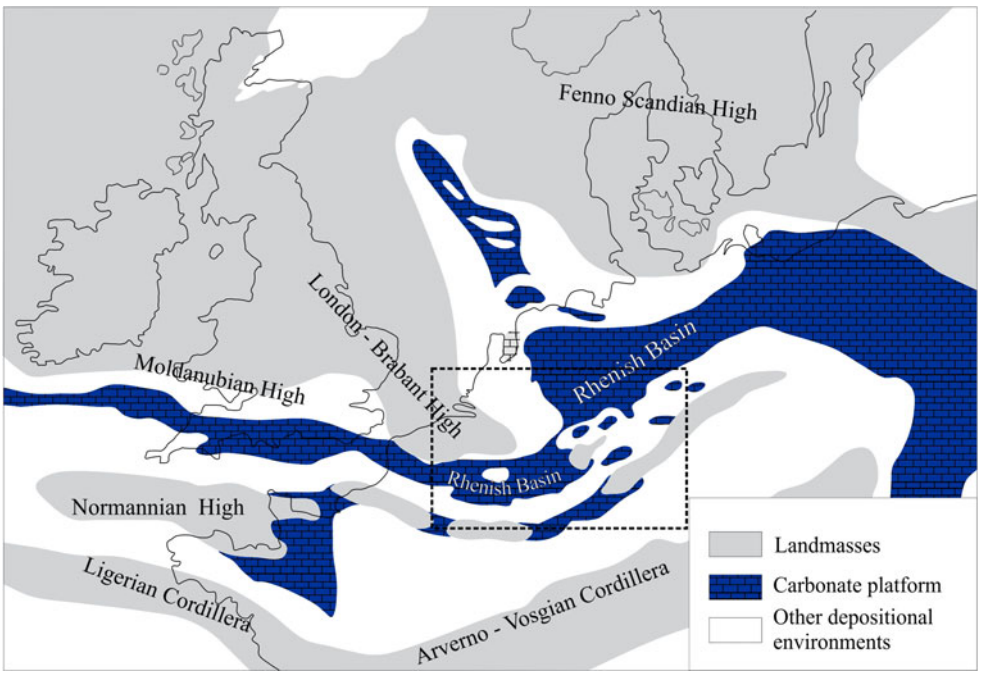

Fig. 1 Paleogeographical setting showing the large carbonate platform developed in northern Europe during the Middle Devonian (modified after Ziegler 1982; McKerrow and Scotese 1990). The enlargement of the *dotted line area* is illustrated in Fig. 2a

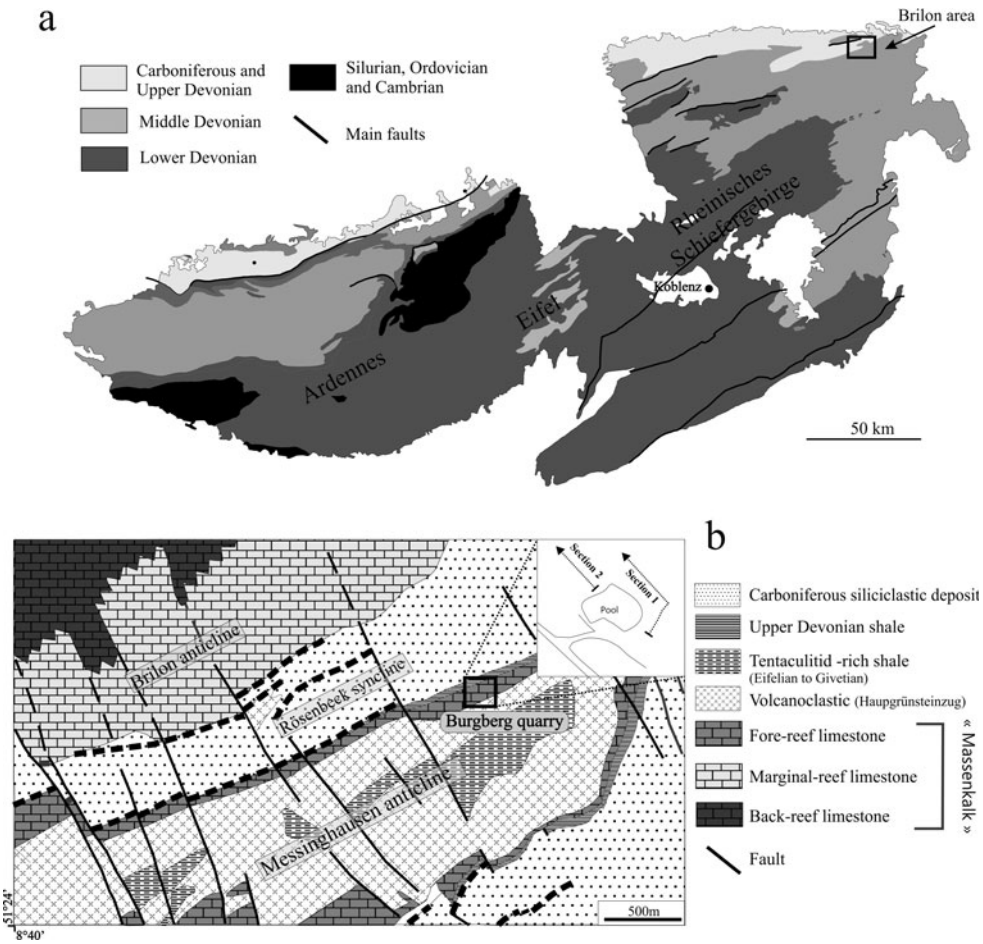

Fig. 2 **a** Location of the Brilon Reef Complex on a simplified geological map of the Rhenohercynian Massif, modified after Wehrmann et al. (2005). **b** Simplified geological map of the Messinghausen anticline with position and enlargement of the Burgberg quarry showing the two studied sections (modified from Ribbert et al. 2006)

carbonate device) connected to a Thermo-Delta^{plus}XL mass spectrometry instrument at the Vrij Universiteit Brussel, Belgium. Samples were calibrated to the NBS19 standard ($\delta^{13}C = 1.95$ promille VPDB).

Results

Biostratigraphy

Several conodont biostratigraphic studies were conducted at the Burgberg quarry (Stritzke 1990; Aboussalam 2003). Nevertheless, they were not sufficient to provide a precise conodont biostratigraphy for this work considering the difficulties for fitting the published lithological columns with our work, as well as the recent changes in conodont terminology. Therefore, additional conodont samples were collected from the Middle Givetian (middle *varcus* Zone) to the Viséan (*bilineatus* Zone). Recognition of this last conodont zone is based on the occurrence of the *Crenistria* Limestone (Nicolaus 1963), a time-equivalent marker horizon (Korn and Kaufmann 2009) of the *bilineatus* Zone within the eastern Rheinisches Schiefergebirge (Warnke 1997). Complete biostratigraphic data resulting from the combination of previously published work (Stritzke 1990, Korn and Kaufmann 2009), new conodont data, and $\delta^{13}C$ measurements around the Frasnian/Famennian boundary (Fig. 6b) allowed the recognition of the Lower and Upper Kellwasser events, which in turn confirms our results for the Frasnian-Famennian boundary.

Description of the section

The succession exposed at Burgberg is overturned and the strata are oriented N110°E with an average dip of 70°SSE. The description of the Burgberg quarry is based on a combination of two sections called section 1 and section 2, respectively (for location of sections, see inset in Fig. 2b), which are partly superposed and provide a stratigraphically continuous succession of strata. The composite section is 117 m thick (Fig. 6) and covers a well-constrained stratigraphic interval (see above 1). The studied section begins with a thick limestone bed (Fig. 4b) overlying a 60-cm-thick outcrop gap. Below the gap, rocks corresponding to the uppermost part of spillitic tuffs of the so-called "Hauptgrünsteinzug" (Clausen and Korn 2008) were found.

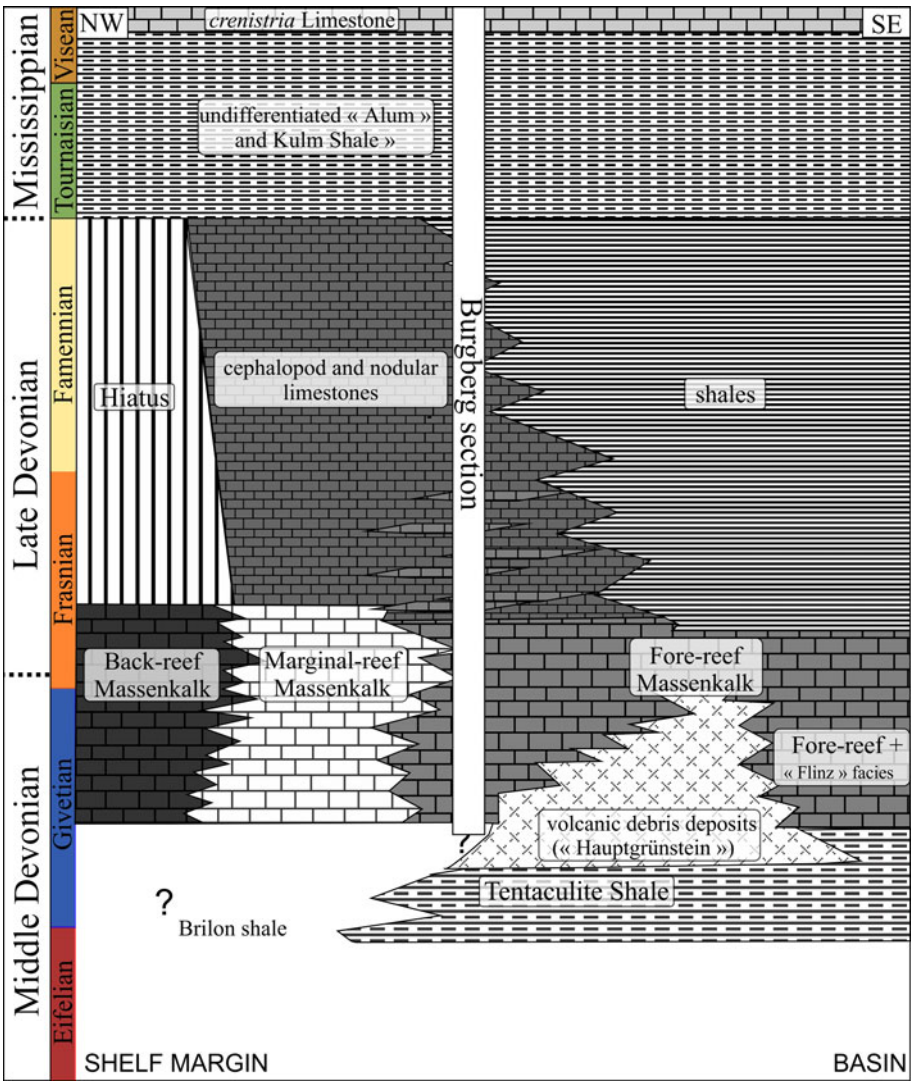

Fig. 3 Stratigraphy and facies relationships of the Brilon Reef Complex area, modified after Malmsheimer et al. (1990) with the stratigraphic interval of the Burgberg section

Five lithological units have been after defined:

- Unit 1 (~4.5 m thick; Figs. 4a, 6). The lower part of this unit (from 0 to 2.15 m) corresponds to several-dm to m-thick dark grey, lenticular-shaped, coarse-bioclastic limestone beds intercalated within black carbonaceous shale layers (Fig. 4a). Bioclasts in the limestone are dominated by several-cm-sized fragments of stromatoporoids, tabulate corals, brachiopods, and crinoids. In the upper part of this unit, a 50-cm-thick alternation of dm-thick dark-grey, fine-grained limestone beds and cm-thick shaly interbeds are observed (from 2.15 to 2.65 m). Within the middle part of the last bed belonging to this unit, a deeply weathered tuff occurs.
- Unit 2 (~55.5 m thick, between 4.5 and 60 m) is mainly composed of grey to blue lenticular to slightly lenticular-bedded bioclastic limestone. The average thickness of the beds is about 60 cm, but m-thick beds occur commonly. A conspicuous character of this unit is the local presence of erosional features on the lower bed surfaces (Fig. 4b). The main bioclasts are crinoids and fragments of reef builders (mainly stromatoporoids). From the middle to the upper part of this unit, stromatoporoid fragments can reach 25 cm in size, while in the lower part these fragments are generally smaller.
- Unit 3 (~29.1 m thick, between 60 and 89.1 m) consists of grey, well-bedded limestone. The main difference with the underlying unit is the strong decrease in the abundance and size of bioclasts, the scarcity of stromatoporoids, and the decrease in bed thickness. Only two massive m-thick beds are observed, located between 79.4 and 82.4 m (bed 166 and 167). These beds are light grey and show common occurrences of spar-filled fractures and irregular cm- to dm-sized cavities filled with calcite.
- Unit 4 (~12.1 m thick, between 89.1 and 112.5 m) corresponds mainly to a several-m-thick succession of

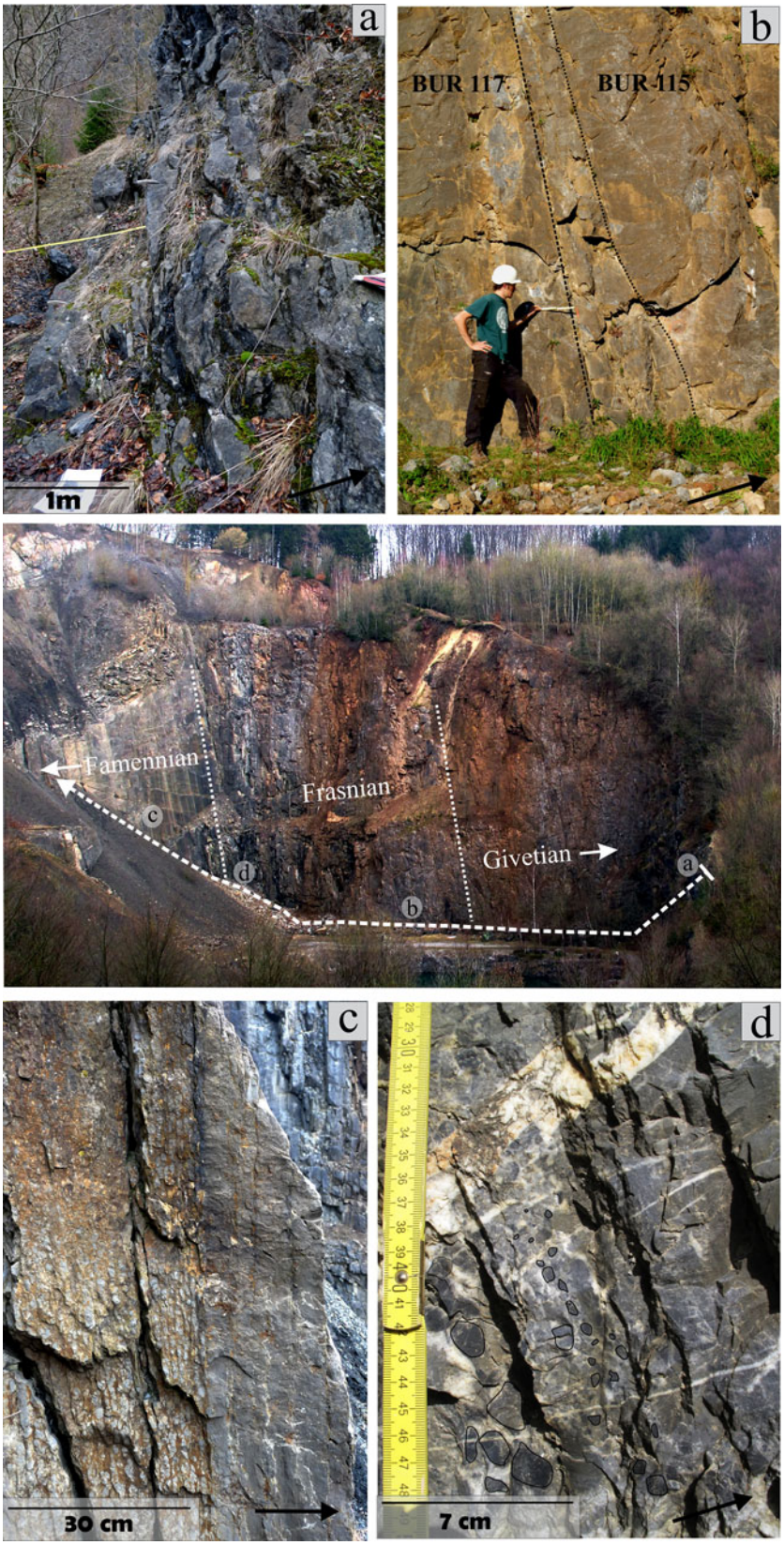

Fig. 4 In the center of the figure: Section 1 of the Burgberg quarry (view from the south) with location of the photographs **a**–**d** (the *arrow* in the *lower right* of the pictures points to the stratigraphic base). **a** Alternation of *thick lenticular-shaped* coarse-grained limestone with thin carbonaceous black shale characterizing the base of the section (microfacies MF3–4). **b** Channel-like structure within bed number 116 (microfacies MF8–9). **c** Thin-bedded limestone passing upward into nodular limestone (MF3). **d** Breccia texture showing coarsening-upward sorting of lithoclasts (delimited by *black lines*) and highly fractured facies (microfacies breccia, MF5)

monotonous light-grey, fine-grained limestone with numerous pressure-solution surfaces (lithologically termed "Flaserkalk"; e.g., Bandel 1974) passing upward into nodular limestone (Fig. 4c). The light-grey, fine-grained limestone is characterized by the common occurrence of thin-shelled bivalves and cephalopods (both shells are several mm in sizes). The nodular limestone is composed of mm- to cm-sized ovoid nodules, which are oriented parallel to the bedding and are highlighted by the contrast of color with the argillaceous dolostone matrix. This uppermost part of the section encompasses the Frasnian-Famennian boundary, located between 96 and 97 m (Fig. 6). A particular character of this unit is the occurrence of a brecciated level between 93 and 94 m (bed number 189; Fig. 6a, b) with inverse grading (Fig. 4d) and black, angular-shaped clasts from 0.5 to 3 cm in size (see Section "Description of the section" for a complete description of this bed). This level and the following ones are affected by numerous calcite-filled veins, crossing the bedding (Fig. 4d).

– Unit 5 (~4.5 m thick, between 112.5 and 117 m) corresponds to the last part of the section and consists mainly of dark-brown to black shale ("Alum and Kulm Shale" of the German literature). In the RS, the Devonian-Carboniferous boundary is marked by the first appearance of the "Lower Alum Shale" overlying fine-grained and nodular limestone (Fig. 5a). The topmost section is marked by the occurrence of three dm-sized limestone beds (so-called *Crenistria* Limestone; Nicolaus 1963; Warnke 1997) (Fig. 5b) named after the occurrence of *Goniatites crenistria*, stratigraphically belonging to the Early Late Viséan (Korn 1996; Korn and Horn 1997). These particular limestone beds are a lithologic marker horizon recognized within the entire eastern RS basin (Korn and Kaufmann 2009).

Microfacies

The field observations and petrographic analyses of thin-sections allowed the discrimination of nine microfacies. The microfacies were compared with other existing microfacies models such as those of Mamet and Préat (1985), Tucker (1974), Wendt and Aigner (1985), May (1994), and Casier and Preat (2007).

MF1: brown to black shale (Figs. 5b, 7a)

This microfacies occurs in the uppermost part of the section between 112.5 and 117 m within Unit 5 and corresponds to dark-brown to black shale with rare limestone nodules. Nodules are cm- to dm-sized and locally appear to coalesce into beds. MF1 is characterized by being laminated and by containing abundant clay particles, common silt-sized quartz grains (average size around 5 μm), and mica flakes. Locally, mm-thick layers enriched in silt-sized quartz occur. Bioclasts are absent.

Interpretation

Shale is generally thought to be deposited in basinal settings (Krebs 1967; Stow and Piper 1984; Piecha 1993; Boulvain et al. 2004) where the main sedimentary process is the settling of suspended particles likely below the storm wave-base (SWB). The absence of bioclasts within this sediment suggests an environment located far from shallow-water influence.

MF2: microbioclastic mudstone to wackestone

This microfacies forms thin-bedded limestone beds with an average thickness of 4 cm, which alternate with nodular/mottled limestone (Fig. 7b, c). It occurs only in the upper part of the section (from 80 to 112.5 m). The thin limestone beds are mostly characterized by the occurrence of pelagic/hemipelagic microfossils, such as goniatites and tentaculitids, thin-shelled pelagic bivalves, entomozoacean ostracods, and sponge spicules. These fossils are scattered in a micritic matrix. The micrite is light grey to grey in color with an average crystal size of around 4 μm. Even if goniatite shells (Fig. 7d) occur, tentaculitids and shells of juvenile pelagic bivalves are the most commonly observed microfossils (Fig. 7e). Locally, fine-grained crinoid debris is common and may be densely packed (local packstone texture). Bioturbation is well developed in this microfacies and is highlighted by selective dolomitization. Dolomitization is common and affects the nodular/mottled fabric (Fig. 7b) mostly where clay minerals are present.

Interpretation

In various sedimentological studies, Devonian cephalopod limestone in Europe has been thought to have accumulated on submarine rises at depths reaching several tens to about 100 m (e.g., Wendt and Aigner 1985; Rabien 1956; Tucker 1973, 1974). Wendt and Aigner (1985) suggested that these carbonates most probably formed during times of reduced sedimentation. A similar setting and faunal composition has also been described from the Gondwana shelf in a Late Devonian section in Thailand (Königshof et al. 2012, cum lit.). The predominance of deep-water fossils such as goniatites, tentaculitids, thin-shelled bivalves, entomozoacean ostracod shells, and sponge spicules points to a hemipelagic/pelagic environmental setting. The very fine grained sediment of microfacies MF2 points to a

low-energy setting, probably located below the SWB where the main sedimentary process is the settling of suspended particles. The vertical evolution from a thin-bedded to a nodular/mottled fabric at the outcrop scale can be easily explained by changes in the bioturbation intensity, carbonate/clay ratio and pressure solution processes. The selective dolomitization commonly occurring in the nodular/mottled fabric is an argument in favor of bioturbation. Gingras et al. (2004) and Clari and Martire (1996) have shown that bioturbation promotes selective dolomitization by increasing the permeability and porosity (e.g., incorporation of organic matter, winnowing of the sediment, remobilization of the clay). Furthermore, according to Möller and Kvingan (1988) and Bathurst (1987), pressure solution processes are also considered to play an important role in the formation of the nodular fabric.

MF3: Carbonaceous microbioclastic wackestone to packstone (Fig. 7f)

This microfacies occurs in up to several cm-thick calcareous shale layers in the first 4 m of the section, alternating with the several-dm-thick dark bioclastic limestone beds of the MF4 (Unit 1, Fig. 4a). They are mainly characterized by common occurrence of bioclast hash (average size $\sim$100 µm), a generally good sorting of the sediment, thin lamination, and black color of the matrix. Most of the bioclasts are undeterminable but locally thin shells of tentaculitids, ostracods, brachiopods, and crinoid debris (average size around 2 µm) can be recognized. Between the fine-grained bioclasts, insoluble residue and clay and silt-sized quartz are observed while matrix is mostly absent; this corresponds to the "stylocumulate texture" of Logan and Semenuik (1976). Locally, mm- to cm-thick irregular and discontinuous layers of MF4 with lower sharp erosional boundary are intercalated in this microfacies (Fig. 7g). As shown below, several-dm-thick layers of MF3 can also be intercalated in this microfacies. Maletz (2006) described a Middle Devonian graptolite fauna (*Dictyonema* and *Ruedemannograptus*) originating from these black calcareous shales from the Brilon reef.

Interpretation

The good sorting of bioclasts, the fine lamination, and the presence of a graptolite fauna suggest a calm sedimentary setting below SWB where deposition is controlled by the settling of particles. Moreover, the presence of thin-shelled tentaculitids, ostracods, bivalves, and brachiopods suggests an open-marine hemipelagic environment. The intercalation of mm- to several-cm-thick layers of MF4 are related to debris-flow deposits originating from the marginal reef area (see MF4), which indicates that episodic downslope transport significantly influenced the Brilon reef.

Fig. 5 *Top of the figure*: Section 2 of the Burgberg quarry (view from the north) showing the transition from the top of the Frasnian, to the lower part of the Carboniferous and location of pictures (**a**) and (**b**). The *arrow* in the *lower right* of the pictures points to the stratigraphic base. **a** Transition from thin-bedded limestone (MF2) with very thin shaly interbeds to the "Lower Alaun Shale" (MF1). This transition corresponds to the petrographic Devonian-Carboniferous boundary. **b** Intercalation of three limestone beds (delimited by *black* and *dotted lines*) called the "*Crenistria* beds" (Rüdiger Stritzke, pers. comm.). These beds contain specimens of *G. crenistria*, a typical goniatite of the Lower Carboniferous

MF4: coarse-grained bioclastic packstone (Fig. 7h)

Bioclastic packstone occurs only in a few dark beds within the first 4 m of the section, and corresponds to the first appearance of limestone after the thick volcanic debris deposits ("Hauptgrünsteinzug"). MF4 alternates with sharp or gradual transition with MF3 carbonaceous microbioclastic packstone levels (Unit 1, Fig. 4a), or occurs as mm- to cm-thick intercalations within MF3 (Fig. 7g). MF4 is a black coarse-bioclastic limestone occurring in several-dm-thick lenticular beds and showing slumping features (thick beds in Fig. 4a). MF4 limestone beds contain stromatoporoid fragments (locally dm-sized), tabulate corals, and brachiopods. Bioclasts are poorly sorted, usually broken, and commonly mm to cm in size. They are represented, in descending order, by crinoids, brachiopods, tabulate corals, bivalves, trilobite shells, bryozoans (Fenestellidae), stromatoporoids, rugose corals, and tentaculitids. Other grains are micritic clasts (average size around 2 mm) and sub-angular mm- to cm-sized lithoclasts of wackestone. Occasionally cm-sized lithoclasts of tuff occur. The allochems commonly show pressure solution structures such as concave-convex and sutured contacts. The matrix of this packstone is a dark-brown micrite, although in some places, insoluble residue and clay occurs between the bioclasts and lithoclasts, while the texture is grain-supported. This corresponds to the "stylocumulate texture" of Logan and Semenuik (1976).

Interpretation

The thickness variations and lenticular shape of the beds (Fig. 4a), the poor sorting and preservation of bioclasts (variable size and shape), the presence of lithoclasts of different origins, and the matrix consisting of micrite and argillaceous material are features commonly linked to debris-flow deposits (Flügel 2004). Regarding the faunal assemblage, two sources of sediment can be distinguished: (1) a shallow-water source indicated by the common presence of reef-builder debris such as stromatoporoids, rugose and tabulate corals, and bryozoans, and (2) a deeper-water source indicated by trilobites, brachiopods, and

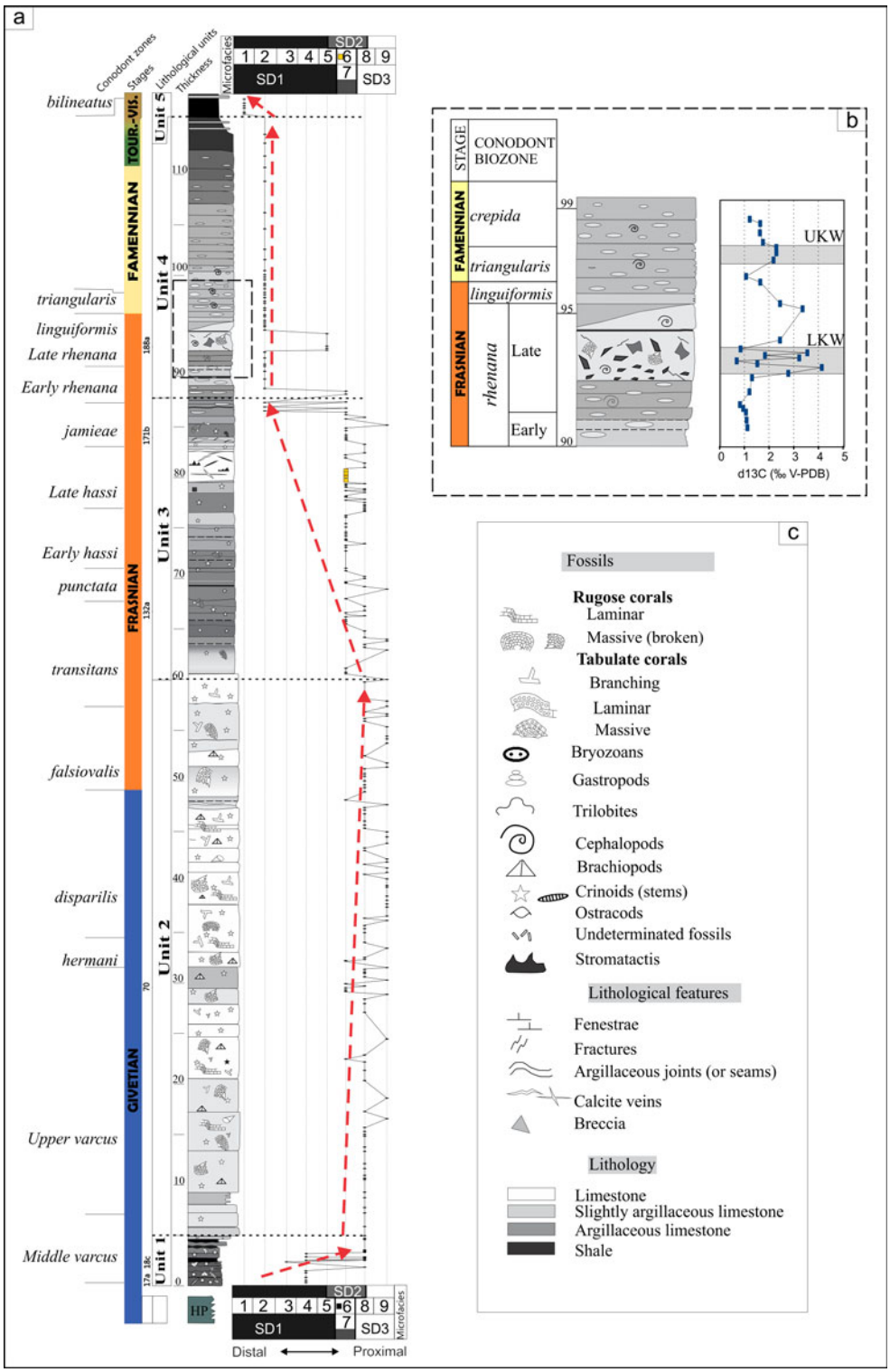

Fig. 6 **a** Schematic sedimentological log showing lithological units (U1–U5) and microfacies curve with main aggrading, prograding, and retrograding trends (*arrows*). The enlargement of the *dotted line area* is illustrated in Fig. 6b. *HP* Hauptgrünstein pyroclastics. **b** $\delta^{13}C$ isotopic trends in the *rhenana* and *triangularis* conodont zones at the Burgberg section. *Grey areas* highlight the Lower (LKW) and Upper (UKW) Kellwasser events. **c** Key of symbols used in this figure

tentaculitids. This mixture between shallow- and deeper-water biota is also commonly observed in debris flows. The intercalations of these thick coarse-grained bioclastic lenticular beds within the black carbonaceous beds (e.g., MF3) indicate deposition below the SWB (see also interpretation of MF3) most probably in a fore-reef setting as indicated by the abundant reefal debris. Volcanic lithoclasts within this microfacies are related to reworking processes of the underlying volcaniclastic rocks. Similar deposits corresponding to the development of reefs on volcaniclastic deposits have been described in the Lahn syncline in the middle v*arcus* Zone at several places (Buggisch and Flügel 1992; Braun et al. 1994; Königshof et al. 2010). The MF4 microfacies corresponds to a debris-flow deposit, which was deposited in an off-reef sedimentary environment and is related to reworking of debris from the newly developed reef on the volcanic substrate of the Hauptgrünstein.

MF5: breccia (Fig. 8a)

At the quarry scale, a single laterally continuous brecciated limestone bed of ~70 cm in thickness was observed in unit 4 between 93 and 94 m (beds 189 and 190), overlying a succession of thin-bedded limestones of MF2. The brecciated bed shows a sharp, slightly erosional contact overlying a fine-grained fabric corresponding to MF2. A coarsening-upward sorting with clasts grading from 0.5–3 cm is observed. Clasts are mainly angular to sub-rounded and consist of peloidal grainstone with tabulate coral debris and clasts of microfacies MF2 and MF6, interpreted as deposited in intermediate reef slope to off-reef carbonate settings. Crinoids and bryozoan debris are also observed. Usually, clasts are matrix-supported but within the upper part of the level, where the largest clasts occur, the fabric is clast-supported with blocky calcite cement.

Interpretation

The dm-thick brecciated level is intercalated between thin-bedded MF2 limestones interpreted as deposited in a quiet depositional setting. However, micro- and macroscopic characters of this microfacies such as the mixture of shallow-marine and deep-marine clasts (mostly matrix-supported), as well as their size, the sharp (slightly erosional) base, and the coarsening-upward nature (Fig. 4d) are indicative of mass-flow or debris-flow deposits. We assume that the larger reefal lithoclasts suffered downslope transport from a shallow platform, which may be related to a rapid sea-level fall.

MF6: Renalcis boundstone (Fig. 8b)

This microfacies was observed only in the upper part of the section, around 80 m within the lithological unit 3. It has been identified as a single m-thick bed intercalated within dm-thick greyish limestone beds of MF7. The massive bed shows common up to several-cm-sized fenestrae and horizontal fractures. The main organisms are *Renalcis* and *Izhella* embedded in a micritic matrix. These calcimicrobes are mostly disseminated but locally they are also densely packed (Fig. 8b). Other observed bioclasts are tabulate corals (around 1 cm in diameter), poorly preserved lamellar stromatoporoid fragments, bryozoan fragments, and tentaculitids. Usually, fenestrae are filled with two generations of cement: a radiaxial calcite at the rim and a blocky sparite in the center. Geopetal infilling by fine micrite at the base of the fenestrae occurs locally.

Interpretation

The abundance of the micritic matrix as well as the good preservation of *Renalcis* and *Izhella* (Fig. 8b), which have been regarded as calcified cyanobacteria by Riding (1991), support a very calm environment below SWB. According to Mamet and Préat (1985), Givetian *Renalcis* in Belgium could create small micritic buildups. The lenticular shape of the bed, its intercalation in bedded limestone MF7, as well as the abundance of *Renalcis* and micritic matrix highlights the depositional character of this microfacies, which corresponds to a small micritic-*Renalcis* mound.

MF7: fine-grained wackestone-packstone with cricoconarid shells and crinoids (Fig. 8c)

This microfacies is mostly observed within Unit 3, in association with microfacies MF8, with sharp transitions (Fig. 8d) or as lenses (mm to several-mm in thickness). Cricoconarids and fine-grained crinoid debris show variable abundance. Cricoconarids (average size around 0.05 mm) are locally concentrated in styliolinid packstone (Fig. 8e). Crinoids are disarticulated and fractured showing an average size of around 0.15 mm even though in some levels they can reach 1 mm. Within these levels, crinoids (Fig. 8f) are commonly oriented parallel to bedding. Other bioclasts are relatively rare and consist of calcispheres, ostracods, entomozoacean ostracods, brachiopods, trilobite fragments, *Amphipora*, stromatoporoids, and *Renalcis* lumps. The average size of these allochems is around 0.15 mm. Bioclasts are commonly associated with rounded peloids with an average size around 0.2 mm. Locally, the proportion of crinoids and cricoconarids is lower and fine-grained peloids dominate the assemblage. Several-mm-sized fenestrae filled with a granular sparite occur. The texture is a wackestone to packstone, although, several-mm- to cm-thick layers of MF8 fine- to coarse-grained grainstones are commonly observed. The lower boundary between the wackestone-packstone texture and the

overlying grainstone is usually sharp and erosional. Episodically, lithoclasts of wackestone-packstone occur within the lower part of the overlying grainstone (Fig. 8g), but the uppermost part of the grainstone layers generally grades into packstone and then wackestone. Dolomitization commonly affected the micrite and is characterized by fine-grained equigranular dolomite crystals.

Interpretation

The common to abundant occurrence of cricoconarid shells embedded in a micritic matrix points to a hemipelagic depositional environment. In this microfacies, however, cricoconarids are associated with shallow-marine bioclasts such as reef-builders, which indicates an occasional input of material from a shallow-marine setting. The mixture of biota could be explained by winnowing of the sediment during high-energy events such as storms. The wackestone-packstone mixture of bioclasts from deep and shallow settings is similar to what is observed in intermediate and distal tempestites described by Wendt and Aigner (1985) and Casier and Preat (2007). The regular occurrence of grainstone layers (MF8) with erosional bases intercalated between the wacke- and packstones also strongly suggests event deposits from turbulent flows such as tempestites or turbidites. The absence of shell layers and the local gradation from grainstone to packstone and then wackestone confirms a turbiditic influence. These sediments were deposited in a hemipelagic intermediate reef slope environment.

MF8: bioclastic and lithoclastic grainstone (Fig. 9 a, b, d)

This microfacies is mainly characterized by the gradual transition from coarse- to fine-grained grainstone, a generally good sorting, and abundant crinoids and micritic clasts of variable size which locally can represent more than 80 % of the assemblage. The average size of micritic clasts is around 0.2 mm, although locally they can reach 2 cm in size. When they are small (0.1–0.2 mm), heterogeneous size distinguishes them from peloids, which show very little variability in size and shape (Tucker and Wright 1990). Large micritic clasts (larger than 0.2 mm) resemble micritized aggregate grains (lumps), and small micritic clasts (0.1–0.2 mm) resemble irregular-shaped peloids ("lithic peloid", Flügel 2004). Lithoclasts of bioclastic grainstone (MF8) or wacke- to packstone (MF7) may occur. They are sub-angular to sub-rounded in shape and usually less than 0.5 mm in size. Another character of MF8 is its common occurrence as several-mm- to cm-thick layers in the wacke- to packstone texture of the MF7. The lower boundary between the wackestone-packstone texture and the overlying MF8 is usually sharp and erosional, and

Fig. 7 Microfacies from the fore-reef deposits (SD1) of the Burgberg section, Germany. Photomicrographs of thin-sections oriented perpendicular to the bedding. *Numbers preceded by "BUR"* correspond to bed numbers. **a** MF1 off-reef deposits: silty shale (BUR 212, transmitted light). **b** MF2 distal reef slope to off-reef: microbioclastic mudstone-wackestone showing nodular/mottled fabric highlighted by the Dickson staining (scanned thin-section BUR 196b). **c** MF2 distal reef slope to off-reef deposit: Nodular texture (scanned thin-section BUR 183b). **d** MF2 distal reef slope to off-reef deposit: fine-grained mudstone with a goniatite shell (BUR 192a, transmitted light). **e** MF2 distal reef slope to off-reef: microbioclastic mudstone with juvenile shells of pelagic bivalves (BUR 197a, transmitted light). **f** MF3 distal reef slope to off-reef deposit: carbonaceous microbioclastic wackestone to packstone overlying coarse-grained crinoidal packstone of MF4 (BUR 18d, transmitted light). **g** MF3 distal reef slope to off-reef deposit: microbioclastic wackestone to packstone showing intercalations of coarse-grained bioclastic packstone of MF4 (scanned thin-section BUR 18d). **h** MF4 distal reef slope to off-reef: coarse unsorted crinoidal packstone with brachiopod shells (BUR 17d, transmitted light)

lithoclasts of MF7 described above mainly occur within the lower part of the overlying grainstone (Fig. 8g). The uppermost part of the grainstone layers generally grades into packstone and then wackestone (Fig. 8d). Crinoids are abundant and crinoidal remains (from 0.2 to 5 mm, with an average size around 1.5 mm) are angular to sub-angular and commonly show syntaxial cement or micritization. Other skeletal grains are rare to common and consist of broken reef builders (*Amphipora*, lamellar and massive stromatoporoids, and tabulate corals), bryozoans, calcispheres, bispheres, ostracods, brachiopods, trilobites, and *Renalcis* lumps. Reef-builder fragments are sub-angular to sub-rounded, range from 0.2–5 mm in diameter, and are commonly surrounded by a micritic envelope (biogenic encrustation of irregular to regular size). Locally, lamination consists of an alternation of light, coarse bioclastic levels dominated by crinoids and darker fine-grained levels dominated by micritic clasts.

Interpretation

The grainstone texture, with a generally good to moderate sorting and the absence of fine-grained particles, suggests a high-energy depositional setting. The presence of crinoids and reef-builder fragments is either related to reworking of the shallower sediments during higher energy events such as storm waves or by downward transport along the proximal fore-reef slope by gravity currents. The occurrence of MF6 and MF7 lithoclasts advocates hydrodynamic conditions strong enough to rework the lithified sediment. The presence of lamination, local fining-upward sequences, and erosional bases strongly support deposition by turbidity currents. MF8 belongs to a turbiditic sequence deposited in the proximal part of a fore-reef environment. Considering the presence of MF7 wackestone-packstone intraclasts, the

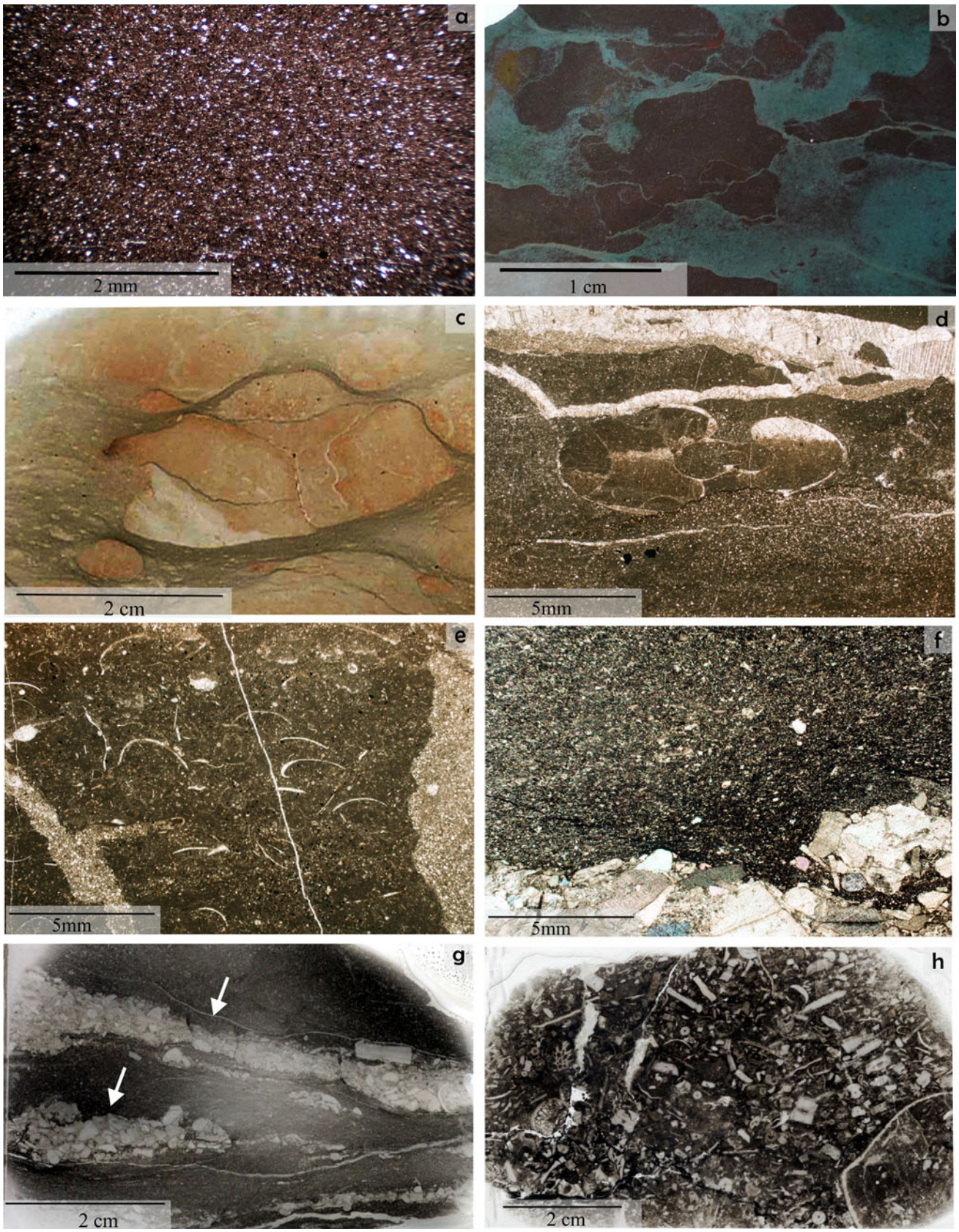

depositional setting was located below the fair-weather wave-base (FWWB) (see interpretation of MF7 above).

MF9: reef-builder rudstone (Fig. 9d)

This microfacies corresponds to well to moderately sorted accumulations of crinoids and reef-builder debris and by the presence of micritic clasts (and/or micritized aggregate grains). The dominant texture of this microfacies is rudstone, and the spaces between large reef-builder fragments are commonly filled by smaller grains cemented by sparite (MF8). Skeletal grains ranging from 0.01 mm to more than 50 mm are mainly represented by crinoid debris (0.1–0.8 mm with an average size about 0.5 mm) and sub-angular to sub-rounded several-cm- to dm-sized reef-builder debris (mostly *Amphipora*, laminar stromatoporoids, and tabulate corals). Porostromate and spongiostromate crusts as well as encrusting stromatoporoids and bryozoans occur. Reef-builder debris is commonly surrounded by a thin irregular-micritized layer. Other skeletal grains were identified as bryozoan debris, fragmented brachiopods, calcispheres, bispheres, rugose coral fragments, and trilobites. Lithoclasts are also commonly observed and are angular to sub-rounded with an average size of 0.25 mm, even though some can reach more than 2 mm. They are either composed of mud-, wacke-, pack-, or grainstone. Locally, pack- and grainstone intraclasts are larger than 2 cm. The main cement of this microfacies is a blocky sparite, although a ferroan sparite calcite may occur locally. Large cavities (centimeter-sized) located under reef builders are showing a succession of radiaxial fibrous cement followed by a blocky sparite. Geopetal micritic infilling also occurs. Generally, MF9 gradually transform into MF8 through a decrease in grain size and in the proportion of reef builders. At the outcrop scale, this microfacies is observed in dm- to m-thick beds showing channel-like structures (Fig. 4b).

Interpretation

The rudstone texture associated with reef-builder debris embedded in a sparitic cement indicates an environment mainly influenced by shallow-water biota (lagoonal such as A*mphipora* and/or reefal such as laminar stromatoporoids). With respect to the good-to-moderate sorting and the common occurrence of syntaxial cement, the MF9 was deposited in a high-energy environment. The presence of reef-builder fragments is either related to reworking of the sediment by storms or by downward transport along the proximal fore-reef slope by turbidity currents. The absence of bivalve shell layers, the homogeneity of biota, and the relatively constant composition of the fauna, suggest deposition influenced by turbidite or grain-flow processes rather than by tempestites. A meter-scale channel-like structure observed in the outcrop (Fig. 4b) and the local gradual transition from coarse rudstone (MF9) to grainstone (MF8) support this assumption. The described sequence is comparable to other sections (May 1994), which have been interpreted to represent parts of allodapic limestone turbidites (Meischner 1964). This microfacies corresponds to the basal part of a proximal limestone turbidite deposited on the proximal part of a fore-reef environment below the FWWB. Regarding the MF8 and MF9 intraclasts exposed in this microfacies, it is suggested that older lithified turbidites were reworked during deposition.

Fig. 8 Microfacies from the fore-reef deposits (SD1 and 2) of the Burgberg section, Germany (continued). Photomicrographs of thin-sections oriented perpendicular to bedding. *Numbers preceded by "BUR"* correspond to bed numbers. **a** MF5 distal reef slope setting: breccia with tabulate coral (Tc), lithoclasts of tabulate coral partially surrounded by black, well-sorted peloidal grainstone (Li-A) and lithoclasts of MF2 (mudstone; Li–B). With numerous calcite-filled veins crossing the breccia texture (scanned polished slab, BUR 189b). **b** MF6 mound facies: *Renalcis*/*Izella* algal aggregates with micritic matrix (BUR 166b, transmitted light). **c** MF7 intermediate reef slope: fine-grained crinoidal packstone with some cricoconarid shells (BUR 146, transmitted light). **d** MF7 intermediate reef slope: transition between MF8 bioclastic grainstone and MF7 fine-grained crinoidal packstone (BUR 122, transmitted light). **e** MF7 intermediate reef slope: styliolinid packstone (BUR 132a, transmitted light). **f** MF7 intermediate reef slope: crinoid debris within a micritic matrix (BUR 57, transmitted light). **g** MF8 proximal reef slope: bioclastic to lithoclastic grainstone with lithoclasts of facies MF7 (BUR 131, transmitted light)

Discussion (Figs. 6a, 10, 11)

Petrographic analyses from the Burgberg section led to the definition of nine microfacies representing a fore-reef to off-reef setting (Fig. 10). In this model, three sedimentary domains (SD) are defined. SD1 corresponds to the most distal setting observed and is characterized by off-reef to distal reef slope sedimentation temporarily influenced by storm and gravity-flows (MF1–5). MF1 and MF2 were located in the most distal setting, while MF3 and MF4 were associated with a slightly more proximal environment. The breccia level (MF5) corresponds to the most proximal setting of SD1. On the intermediate reef slope (SD2), sediments are composed of a mixture of deeper-water autochthonous and shallow-water allochthonous debris (MF7), and in this setting *Renalcis* mound-like structures developed locally (MF6). On the upper reef slope (SD3), the most proximal facies of the succession are observed (MF8-9).

The temporal changes in microfacies point to five main paleoenvironmental trends, which correspond to the five lithological units defined in the Burgberg section. Unit 1 marks the Middle Givetian (middle *varcus* Zone) initiation

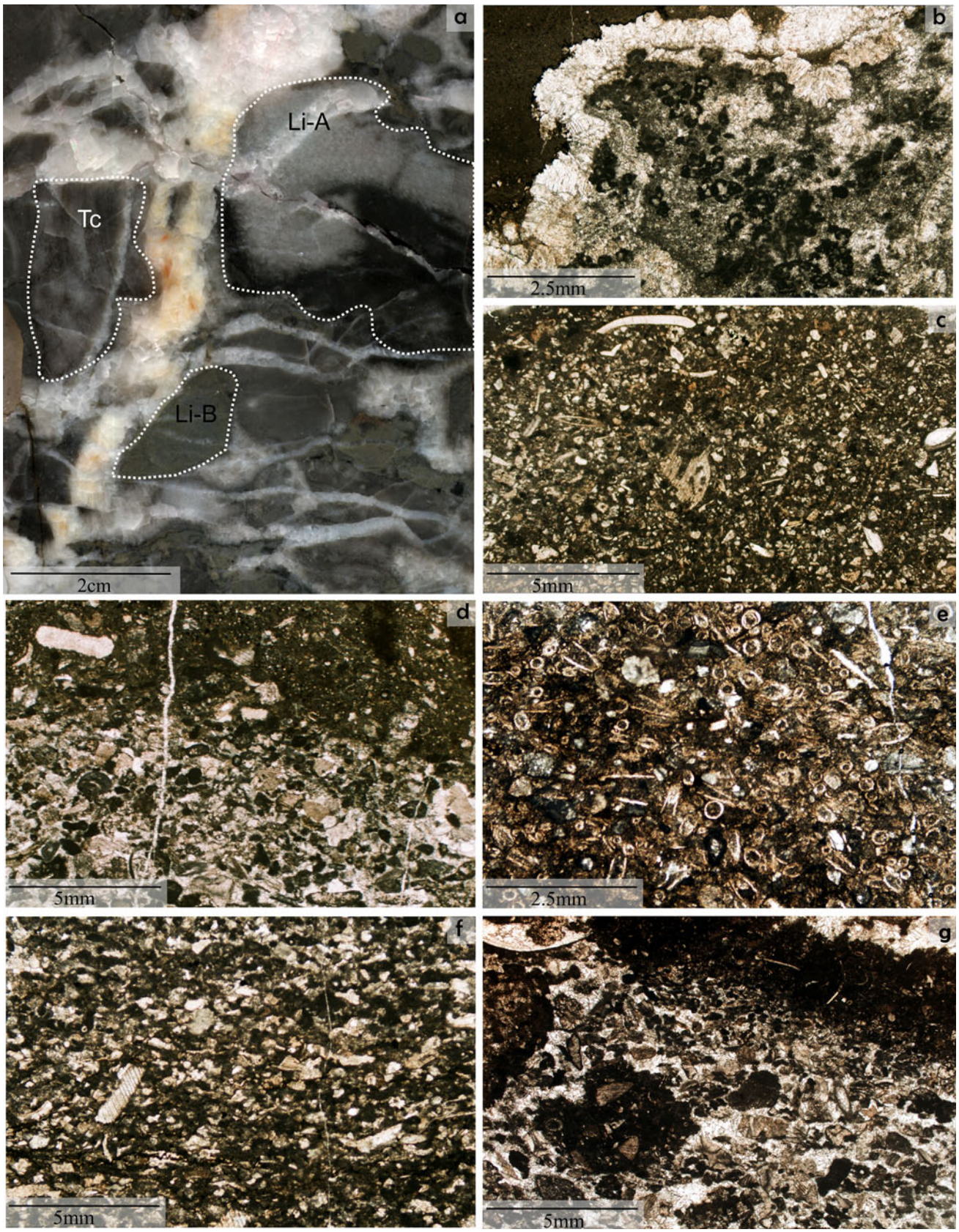

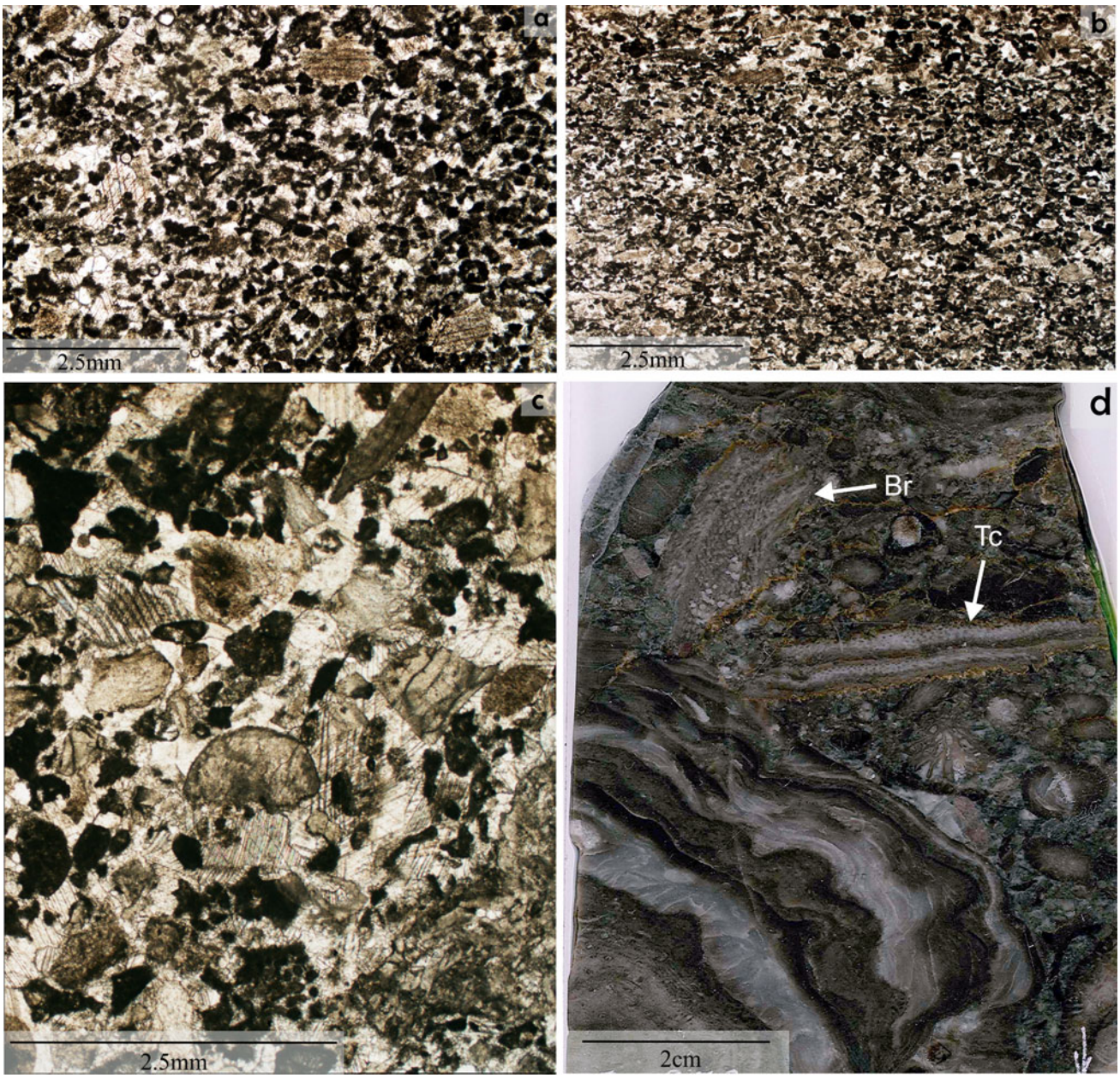

Fig. 9 Microfacies from the fore-reef deposits (SD3) of the Burgberg section, Germany (continued). Photomicrographs of thin-sections oriented perpendicular to bedding. *Numbers preceded by "BUR"* correspond to bed numbers. **a** MF8 proximal reef slope: fine-grained peloidal grainstone (BUR 36, transmitted light). **b** MF8 proximal reef slope: fine-grained lithic peloidal grainstone with crinoids (BUR 128, transmitted light). **c** MF9 proximal reef slope: coarse-grained grainstone with numerous dark-colored lithoclasts (BUR 97c, transmitted light). **d** MF9 proximal reef slope facies: reef-builder rudstone with bryozoan (Br), tabulate coral (Tc), and, in the *lower-left part*, multiple stromatoporoid and bryozoan crusts (scanned thin-section, BUR 73)

of the reefal platform on volcanic debris deposits of the "Hauptgrünstein" (Fig. 11a). A middle *varcus* age was also assigned by Malmsheimer et al. (1990) for the first debris flows covering large areas in the southeast margin of the reef complex. During Middle and Late Givetian times, numerous reef structures developed related to submarine volcanoes in the Rheinisches Schiefergebirge and the Harz Mountains (e.g., Königshof et al. 1991, 2010; May 1993; Gischler 1995, 1996; Nesbor 2004). The onset of carbonate production in the Burgberg area is thus likely related to the end of the volcanic activity in basinal areas, which gave rise to the development of reefal structures and corresponding off-reef deposits. The reefal origin of the debris flow occurring in Unit 1 is linked to the onset of reef growth in the Burgberg area. Furthermore, according to Aboussalam and Becker (2011), the black color of the

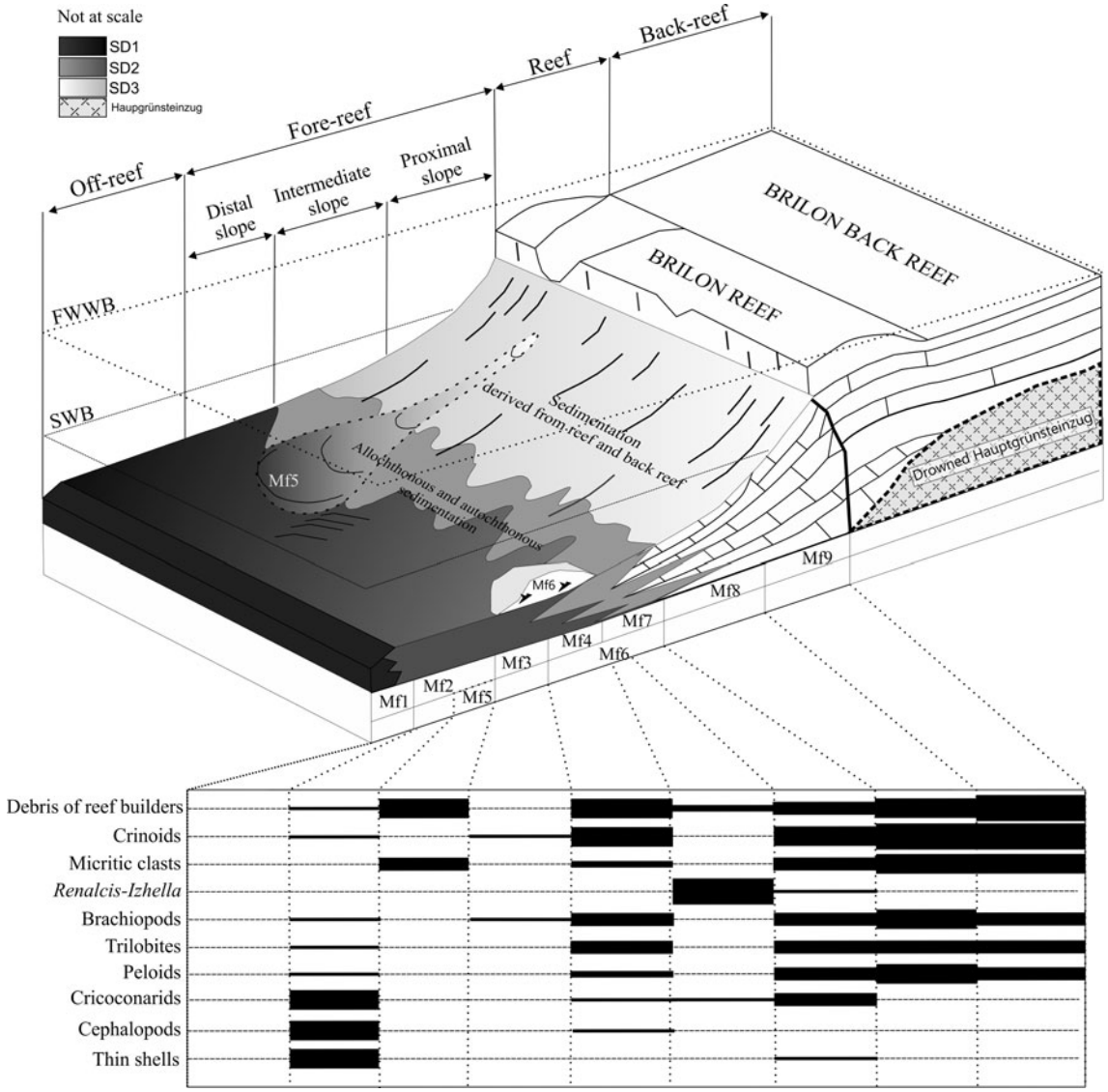

Fig. 10 Sedimentary model of the Burgberg succession showing the relative position of the nine microfacies described. The Brilon reef and the back-reef have not been observed in the Burgberg section but are inferred from literature and from the nature of the debris observed. The *lower part* of the figure depicts the distribution of the main fossils and allochems throughout the different microfacies

sediment (Figs. 4a, 7f–h) occurring in the lower part of the Burgberg section is most likely related to the Taghanic Event at the end of the Middle Givetian, which triggered oxygen-depleted conditions in distal slope environment. This first unit records an abrupt shallowing-upward, which is related to the transition from the distal reef slope (Unit 1; MF3, MF4) to the proximal reef slope of the second unit (Unit 2; MF7, MF8 and MF9). The microfacies curve corresponding to Unit 2 mainly records a prograding trend in the intermediate to proximal reef slope setting (MF7, MF8, and MF9), which is marked by the progressive increase in the proportion of MF9 in comparison to MF7-8 through the top of the Unit 2. A progradational pattern was also recognized by Machel (1990) and Städter and Koch (1987) in the south of the Brilon reef towards the Upper Givetian and can be linked with the global second-order sea-level rise recognized by Johnson et al. (1985) and Haq and Schutter (2008) during the Givetian. Relative sea-level rise may also have been influenced by cooling-related subsidence of the volcanic bodies. The higher proportion of MF9 (interpreted as the most proximal setting) through the top of Unit 2 (*disparilis* and *falsiovalis* conodont zones) marks a higher influence of shallow-water habitats. During this interval, the rate of carbonate accumulation exceeded the rate of subsidence, resulting in the progradation of shallow-water depositional environments over deeper-water ones. Climax of the reefal development and thus the maximum of progradation towards the southeastern part of

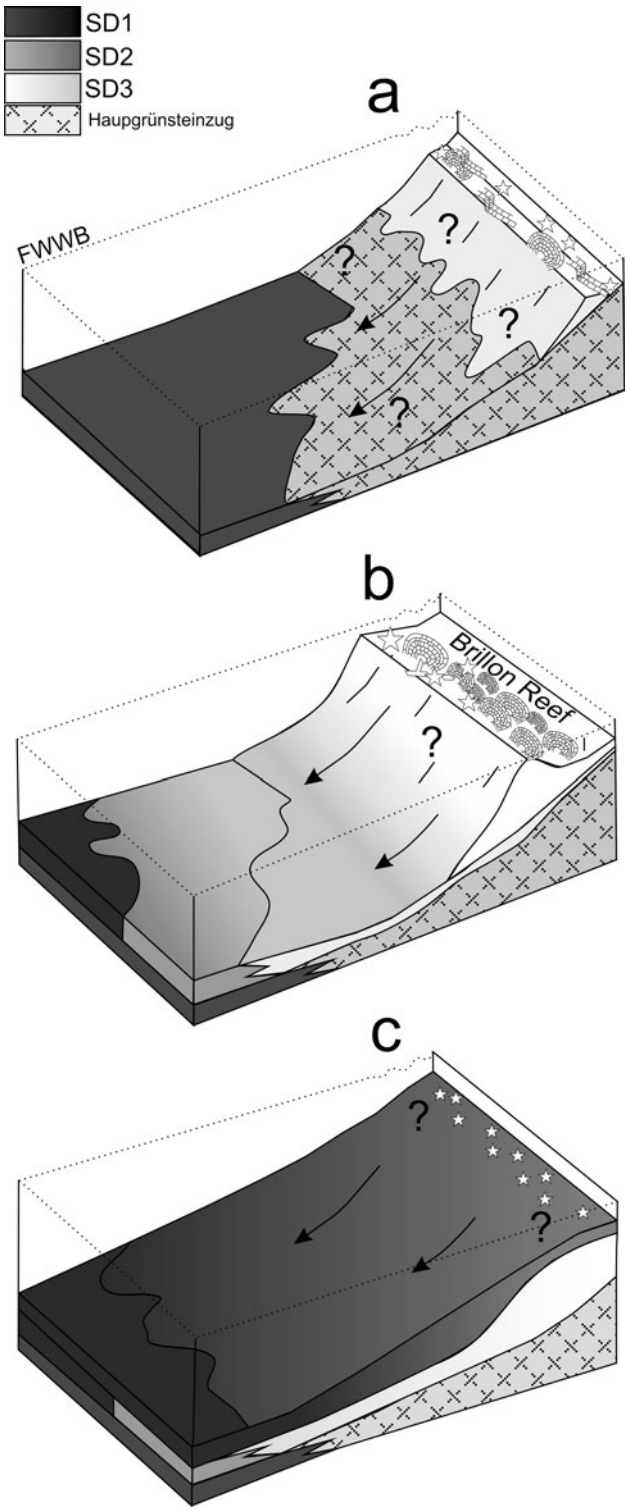

◀ **Fig. 11** Temporal evolution of the southeastern fringe of the Brilon Reef Complex from the Middle Givetian to the Viséan. **a** Unit 1: deposition of MF3-4 in the Burgberg area, with alternating microbioclastic wackestone and packstone including reefal debris. This corresponds to the onset of the carbonate production and the initial phase of reef growth on the "Hauptgrünstein" volcaniclastics during the middle *varcus* Zone. **b** Unit 2: deposition of MF7 (SD2) and MF8-9 (SD3) in the Burgberg area, with bioclastic rudstone and grainstone with abundant reefal debris and fine-grained bioclastic packstone. This corresponds to the extension of the Brilon reef from the middle *varcus* Zone to the *falsiovalis* Zone. **c** Units 4 and 5: deposition of MF1-2 (SD1) in the Burgberg area with thin-bedded limestone and dark shale. This corresponds to the deepening of the Burgberg area after the demise and drowning of the Brilon Reef Complex at the Frasnian-Famennian boundary. *Arrows* represent downslope transport of reefal debris towards the fore-reef area. Key of symbols in Fig. 6c

the Brilon Reef Complex extended from the Late Givetian to the Early Frasnian. The long-lasting and significant influence of the shallow-water habitats in the fore-reef setting of Burgberg, mainly characterized by *Amphipora*, tabulate corals, and stromatoporoids, indicates that conditions were favorable for reef development during the equivalent period of time in the shallow-water area of the Brilon Reef Complex (Fig. 11b). In the reef complexes of the Australian Canning Basin (Playford 1980), the Late Givetian to Early Frasnian time span is also characterized by an increasing amount of reefal material deposits in the marginal slope setting and has been interpreted as the result of an increase in the rate of transgression. The overlying third unit corresponds to a deepening-upward trend extending from the *transitans* to *jamieae* conodont zones, which is characterized by a progressive decrease in deposits of shallow-water origin (MF8 and MF9). Furthermore, an increase in the amount of hemipelagic/pelagic biota associated with fine-grained sediments (MF7) is visible. The changes in biota are related either to an increase in the global sea-level rise, an increase in the subsidence, or to a combination of both which finally led to the progressive retrogradation and back-stepping of the Brilon Reef Complex and corresponding off-reef deposits. This back-stepping has also been recorded in the fore-reef setting of the Australian Canning Basin (Playford 1980) and in the Canadian Rocky Mountains (Whalen 2000) around the Middle to Late Frasnian. Back-stepping of carbonate platforms at that time is a general trend recorded on a global scale and it is commonly correlated with several Frasnian pulses in the eustatic sea-level rise (Johnson et al. 1985; T-R cycle IId). However, the global sea-level fall documented by Haq and Schutter (2008) for the Frasnian stage is inconsistent with the deepening trend recorded in our data. The development of *Renalcis* mound-like structures (MF6) within the fore-reef area of the Brilon Reef Complex may be correlated with the progressively decreasing influx of reef debris to open-marine reef slope setting, which may confirm an increasing distance between the Burgberg fore-reef depositional setting and the shallow-water areas. The deepening trend characterizing the Unit 3 ends within the *jamieae* conodont Zone with sediments belonging to the distal reef slope to off-reef setting (MF2). The following aggrading trend (Unit 4) in the distal reef slope to off-reef setting is characterized by thin-

bedded nodular and cephalopod-rich limestones (MF2) extending from the Late Frasnian to the Late Famennian stages. The breccia level (MF5) in the lower part of Unit 4 represents a strong shallowing-upward episode within the general aggrading trends in off-reef setting. The biostratigraphic position of this breccia in the late *rhenana* conodont Zone as well as the major positive $\delta^{13}C$ excursions (amplitude +4.14 ‰ and +3.56 ‰; Fig. 6b), correspond to the Lower Kellwasser Event (LKW). Similar positive $\delta^{13}C$ excursions were described from other European sections (Buggisch and Joachimski 2006). The Upper Kellwasser Event is also present in our section (Fig. 6b). The $\delta^{13}C$ excursions are usually associated with black shale levels and are interpreted to correspond to deepening events, although our breccia level, associated with high $\delta^{13}C$ values, is likely to be related to a shallowing event. This breccia level could thus correspond to the strong sea-level fall occurring worldwide (Johnson et al. 1985; Wendt and Belka 1991; Chen et al. 2002; Bond and Wignall 2008) after the Lower Kellwasser Event in the Late Frasnian, which generated exposure and collapse of shallow platform settings (e.g., George and Powell 1997; Bond et al. 2004). A global eustatic sea-level fall associated with the end of the Frasnian is recognized in many areas, such as on the East European Platform (Alekseev et al. 1996; Antoshkina 2006), in Western Canada (Geldsetzer et al. 1993) and in Southern China (Chen and Tucker 2004). The high values of $\delta^{13}C$ recorded in the breccia level suggest a reworking of the Lower Kellwasser sediments triggered during the deposition of this breccia level. The reef-derived bioclasts in the breccia level are the last occurrence of the shallow-water influxes within the Burgberg section and therefore confirm the existence of shallow-water areas south of the Brilon Reef Complex, at least until the late *rhenana* conodont Zone. For comparison, reef development in the Harz Mountains (Iberg reef) ranges from the *varcus* conodont Zone to the *rhenana* conodont Zone (Franke 1973). The dominance of MF2 within Unit 4 indicates the end of the shallow-water influx, which seems to be related to the demise and drowning of the shallow-water habitats in the Burgberg area as a result of the Late Frasnian sea-level rise. According to Eder and Franke (1982) and Johnson et al. (1985), the Late Frasnian eustatic sea-level rises caused the drowning of carbonate platforms on a global scale. They appear to be connected to the Kellwasser event interval at the end of the Frasnian, which is considered to be one of the major extinction events of the Phanerozoic (Sepkoski 1995) and marks the end of the Devonian reef communities. The beginning of the last unit (Unit 5; Fig. 6a) records a significant deepening trend related to the transition from bedded cephalopods and nodular limestone (MF2) to poorly oxygenated pelagic shale of MF1. In the Burgberg section, pelagic shale extends from the Late Famennian to the Viséan (Fig. 11c), which indicates poorly oxygenated bottom water conditions in the Burgberg area during a long stratigraphic interval. A similar aggrading facies development has been described in other parts of the Rhenish Massif, such as the Harz Mountains (e.g., Gischler 1996). The occurrence of the *Crenistria* Limestone beds (Fig. 5b) in the topmost part of the section corresponds to a change in the environmental conditions dominating in the basin. Indeed, the *Crenistra* Limestone beds are interpreted as a phases of bottom water oxygenation (Warnke et al. 1997).

Conclusions

(1) The Burgberg section provides an outstanding continuous succession of about 40 Ma in a fore-reef facies and can serve as an important contribution to the understanding of reef development in the Mid-Paleozoic. The stratigraphic framework of the entire section is well documented by conodont biostratigraphy.

(2) The section ranges from the Middle Givetian (middle *varcus* Zone) to the Viséan (*bilineatus* Zone) and contains the global Kellwasser events as shown by biostratigraphic and carbon-isotope data.

(3) The main sedimentary processes documented in the Burgberg section are gravity flows (turbidite, debris, and grain flows) and pelagic sedimentation (settling). Reworking by storms and bioturbation are locally important.

(4) Based on a detailed study of the microfacies, the development of the off-reef facies and corresponding Brilon reef can be reconstructed. The major evolutionary phases are (a) initial development of the Brilon reef on top of volcanic deposits which started within the middle *varcus* conodont Biozone, (b) the establishment of the reef structure lasting from the Middle Givetian to Early Frasnian with a culmination recorded from the *disparilis* to *falsiovalis* conodont biozones, (c) the stepwise withdrawal of the reef development from the Middle to the Late Frasnian, (d) the end of the reef development as a result of the global Kellwasser events, and finally (e) significant deepening of the Burgberg area starting in the Late Famennian, characterized by pelagic shale sedimentation overlying nodular limestones.

(5) The detailed sedimentological study of the Burgberg section demonstrates the potential of fore-reef sequences for the reconstruction of major paleoenvironmental changes that can occur in shallow-water reefal habitats.

Acknowledgments Financial support for this project from the sedimentary laboratory of the University of Liège is gratefully acknowledged. The authors would like to thank Philippe Claeys and David De Vleeschouwer (Earth System Sciences, Vrije Universiteit

Brussel) for the instrumental help provided for the stable isotope measurements. Many thanks to Rüdiger Stritzke for all the information and comments provided for conodont investigation. This paper is a contribution to IGCP 580 "Application of magnetic susceptibility in paleoenvironmental reconstruction" and to IGCP 596 "Climate change and biodiversity patterns in the Mid-Palaeozoic". Helpful comments from Dr. Thomas Suttner (Karl-Franzens University of Graz, Austria) and an anonymous journal reviewer are gratefully acknowledged.

References

Aboussalam ZS (2003) Das" Taghanic-Event" im höheren Mitteldevon von West-Europa und Marokko. Münstersche Forsch Geol Paläont 97:1–332

Aboussalam ZS, Becker RT (2011) The global Taghanic biocrisis (Givetian) in the eastern Anti-Atlas, Morocco. Palaeogeogr Palaeoclimatol Palaeoecol 304:136–164

Alekseev AS, Kononova LI, Nikishin AM (1996) The Devonian and Carboniferous of the Moscow Syneclise (Russian Platform): stratigraphy and sea level changes. Tectonophysics 268:149–168

Antoshkina AI (2006) Palaeoenvironmental implications of Palaeomicrocodium in Upper Devonian microbial mounds of the Chernyshev Swell, Timan-northern Ural region. Facies 52:611–625

Bacelle L, Bosellini A (1965) Diagrammi per la stima visiva della composizione percentuale nelle rocce sedimentarie. Ann Univ Ferrara Sez 9 Sci Geol Paleont 1:59–62

Bandel K (1974) Deep-water limestones from the Devonian-Carboniferous of the Carnic Alps, Austria. Spec Publ Int Assoc Sediment 1:93–115

Bär P (1968) Die ober-devonisch/unter-karbonische Schichtlücke über dem Massenkalk des Briloner und Messinghäuser Sattels (Ost-Sauerland). N Jb Geol Paläont Abh 131:263–288

Bathurst RGC (1987) Diagenetically enhanced bedding in argillaceous platform limestones: stratified cementation and selective compaction. Sedimentology 34:749–778

Bond DPG, Wignall PB (2008) The role of sea-level change and marine anoxia in the Frasnian–Famennian (Late Devonian) mass extinction. Palaeogeogr Palaeoclimatol Palaeoecol 263:107–118

Bond DPG, Wignall PB, Racki G (2004) Extent and duration of marine anoxia during the Frasnian-Famennian (Late Devonian) mass extinction in Poland, Germany, Austria and France. Geol Mag 141:173–193

Boulvain F, Cornet P, da Silva AC, Delaite G, Demany B, Humblet M, Renard M, Coen-Aubert M (2004) Reconstructing atoll-like mounds from the Frasnian of Belgium. Facies 50:313–326

Braun R, Oetken S, Königshof P, Kornder L, Wehrmann A (1994) Development and biofacies of reef-influenced carbonates (Lahnsyncline, Rheinisches Schiefergebirge). Cour Forschungsinst. Senckenberg 169:351–386

Brinckmann J (1981) Projekt Rhenoherzynikum: Untersuchung der Metallverteilung in geosynklinalen Sedimenten des Rhenoherzynikums in stratiformen Konzentrationen; Bericht über das Kernbohrprogramm im Briloner Riffkalk-Komplex. Bundesanstalt für Geowissenschaften und Rohstoffe

Buggisch W, Flügel E (1992) Mittel- bis oberdevonische Karbonate auf Blatt Weilburg (Rheinisches Schiefergebirge) und in Randgebieten: Initialstadien der Riffentwick-lung auf Vulkanschwellen. Geol Jb Hessen 120:77–97

Buggisch W, Joachimski MM (2006) Carbon isotope stratigraphy of the Devonian of central and southern Europe. Palaeogeogr Palaeoclimatol Palaeoecol 240:68–88

Casier J, Preat A (2007) Ostracodes et lithofacies du stratotype de la limite Devonien moyen/Devonien superieur (Puech de la Suque, Montagne Noire, France). Bull Soc Geol France 178:293–304

Chen D, Tucker M (2004) Palaeokarst and its implication for the extinction event at the Frasnian–Famennian boundary (Guilin, South China). J Geol Soc Lond 161:895–898

Chen D, Tuker M, Shen Y, Yans J, Preat A (2002) Carbon isotope excursions and sea-level change: implications for the Frasnian–Famennian biotic crisis. J Geol Soc Lond 159:623–626

Clari P, Martire L (1996) Interplay of cementation, mechanical compaction, and chemical compaction in nodular limestones of the Rosso Ammonitico Veronese (Middle-Upper Jurassic, northeastern Italy). J Sediment Res 66:447–458

Clausen CD, Korn D (2008) Höheres Mitteldevon und Oberdevon des nördlichen Rheinischen Schiefergebirges (mit Velberter Sattel und Kellerwald). In: Deutsche Stratigraphische Kommission (eds) Stratigraphie von Deutschland VIII. Devon. Schriftenreihe dtsch Ges Geowiss Heft 52:439–481

Copper P (2002) Silurian and Devonian reefs: 800 million years of global greenhouse between two ice ages. In: Kiessling W, Flügel E, Golonka J (eds) Phanerozoic reef patterns. SEPM Spec Publ, vol 72, pp 181–238

Dickson J (1965) A modified staining technique for carbonates in thin section. Nature 205:587

Dunham RJ (1962) Classification of carbonate rocks according to depositional texture. Mem Am Assoc Petrol Geol 1:108–121

Eder W, Franke W (1982) Death of Devonian reefs. N Jb Geol Paläont Abh 163:241–243

Embry AF, Klovan JE (1972) Absolute water depth limits of Late Devonian paleoecological zones. Geol Rundsch 61:672–686

Erben HK (1962) Zur Analyse und Interpretation der rheinischen und hercynischen Magnafazies im Devon. In: Erben HK (ed) International Arbeitstagung über die Silur/Devon Grenze und die Stratigraphie von Silur und Devon. Symposium Band, Schweizerbart, Stuttgart, pp 42–61

Flügel E (2004) Microfacies analysis of carbonate rocks. Analysis, interpretation and application. Springer, Berlin Heidelberg New York

Franke W (1973) Fazies, Bau und Entwicklungsgeschichte des Iberger Riffes (Mitteldevon bis Unterkarbon III NW-Harz, W-Deutschland). Geol Jb A 11:27–31

Geldsetzer HHJ, Goodfellow WD, McLaren DJ (1993) The Frasnian-Famennian extinction event in a stable cratonic shelf setting: Trout River, Northwest Territories, Canada. Palaeogeogr Palaeoclimatol Palaeoecol 104:81–89

George AD, Powell CMA (1997) Paleokarst in an Upper Devonian reef complex of the Canning basin, western Australia. J Sediment Res 67:935–944

Gingras MK, Pemberton SG, Muelenbachs K, Machel H (2004) Conceptual models for burrow-related, selective dolomitization with textural and isotopic evidence from the Tyndall Stone, Canada. Geobiology 2:21–30

Gischler E (1995) Current and wind induced facies patterns in a Devonian atoll: Iberg Reef, Harz Mts. Germany. Palaios 10:180–189

Gischler E (1996) Late Devonian-early Carboniferous deep-water coral assemblages and sedimentation on a Devonian seamount: Iberg Reef, Harz Mts. Germany. Palaeogeogr Palaeoclimatol Palaeoecol 123:297–322

Haq BU, Schutter SR (2008) A chronology of Paleozoic sea-level changes. Science 322:64–68

House MR (1985) Correlation of Mid-Palaeozoic ammonoid evolutionary events with global sedimentary perturbations. Nature 313:17–22

Johnson JG (1970) Taghanic onlap and the end of North American Provinciality. Geol Soc Am Bull 81:2077–2106

Johnson JG, Klapper G, Sandberg CA (1985) Devonian eustatic fluctuations in Euramerica. Geol Soc Am Bull 96:567–587

Jux U (1960) Die devonischen Riffe im Rheinischen Schiefergebirge. N Jb Geol Paläont Abh 110:186–258

Königshof P, Gewehr B, Kornder L, Wehrmann A, Braun R, Zankl H (1991) Stromatoporen-Morphotypen aus einem zentralen Riffbereich (Mitteldevon) in der südwestlichen Lahnmulde. Geol Palaeont 25:19–35

Königshof P, Nesbor HD, Flick H (2010) Volcanism and reef development in the Devonian: a case study from the Lahn syncline, Rheinisches Schiefergebirge (Germany). Gondwana Res 17:264–280

Königshof P, Savage N, Lutat P, Sardsu A, Dopieralska J, Belka Z, Racki G (2012) Late Devonian sedimentary record of the Palaeotethys Ocean—the Mae Sariang succession, northwestern Thailand. J Asian Earth Sci 52:146–157. doi:10.1016/j.jseaes.2012.03.006

Korn D (1996) Revision of the Late Visean goniatite stratigraphy. Ann Soc Geol Belg 117:205–212

Korn D, Horn K (1997) The Late Visean (early Carboniferous) goniatite stratigraphy in the South Portuguese Zone, a comparison with the Rhenish Massif. Newsl Stratigr 35:97–113

Korn D, Kaufmann B (2009) A high-resolution relative time scale for the Viséan Stage (Carboniferous) of the Kulm Basin (Rhenish Mountains, Germany). Geoll J 44:306–321

Krebs W (1967) Reef development in the Devonian of the eastern Rhenish Slate Mountains, Germany. In: Oswald DH (ed) International symposium on the Devonian system, vol 1. Alberta Society of Petroleum Geologists, Calgary, pp 295–306

Krebs W (1971) Devonian reef limestones in the eastern Rhenish Schiefergebirge. Sedimentology of parts of Central Europe guidebook, 8th international sedimentology congress, Heidelberg, pp 45–81

Krebs W (1974) Devonian carbonate complexes of central Europe. In: Laporte LF (ed) Reefs in time and space. SEPM Spec Publ, vol 18, pp 155–208

Kroner U, Hahn T, Romer RL, Linnemann U (2007) The Variscan orogeny in the Saxo-Thuringian zone—heterogenous overprint of Cadomian/Palaeozoic peri-Gondwana crust. In: Linnemann U, Nance RD, Kraft P, Zulauf G (eds) The evolution of the Rheic Ocean: From Avalonian-Cadomian active margin to Alleghenian-Variscan collision. Geol Soc Am Spec Pap 423: 153–172

Logan BV, Semenuik V (1976) Dynamic metamorphism: processes and products in Devonian carbonate rocks, Canning Basin, Western Australia. Geol Soc Australia Spec Publ 138

Machel H-G (1990) Faziesinterpretation des Briloner Riffs mit Hilfe eines Faziesmodells für devonische Riffkarbonate. Geol Jb D 95:43–83

Maletz J (2006) Middle Devonian dendroid graptolites from the Brilon Reef area (Rheinisches Schiefergebirge, Germany). Paläont Z 80:221–229

Malmsheimer KW, Mensink H, Stritzke R (1990) Beginn der Riffschutt-Produktion und Knollenkalk-Sedimentation in Südosten des Briloner Riffes/Ostsauerland. Geol Jb D 95:177–182

Mamet B, Préat A (1985) Sur la présence de *Palaeomicrocodium* (Algue?, Incertae sedis?) dans le Givétien inférieur de Belgique. Geobios 18:389–395

May A (1993) Stratigraphie, Stromatoporen-Fauna und Palökologie von Korallenkalken aus dem Ober-Eifelium und Unter-Givetium (Devon) des nordwestlichen Sauerlandes (Rheinisches Schiefergebirge). Geol Paläont Westfalen 24:1–93

May A (1994) Microfacies controls on weathering of carbonate building stones: Devonian (northern Sauerland, Germany). Facies 30:193–208

McKerrow WS, Scotese CR (1990) Palaeozoic palaeogeography and biogeography. Geol Soc Lond Mem 12:1–433

Meischner KD (1964) Allodapische Kalke. Turbidite in riff-nahen Sedimentations-Becken. Developm Sediment 3:156–191

Möller NK, Kvingan K (1988) The genesis of nodular limestones in the Ordovician and Silurian of the Oslo Region (Norway). Sedimentology 35:405–420

Nesbor HD (2004) Paläozoischer Intraplattenvulkanismus im östlichen Rheinischen Schiefergebirge—Magmenentwicklung und zeitlicher Ablauf. Geol Jb Hessen 131:145–182

Nicolaus HJ (1963) Zur Stratigraphie und Fauna der *crenistria*-Zone im Kulm des Rheinischen Schiefergebirges. Beih Geol Jahrb 53:1–246

Paeckelmann W (1922) Der mitteldevonische Massenkalk des Bergischen Landes. Preuss Geol Landesanst Abh 91:1–112

Paeckelmann W (1936) Geologische Karte von Preussen 1: 25000. Blatt Brilon (2659)

Pettijohn FJ, Potter PE, Siever R (1972) Sand and sandstone. Springer, Berlin Heidelberg New York

Piecha M (1993) Stratigraphie, Fazies und Sedimentpetrographie der rhythmisch und zyklisch abgelagerten, tiefoberdevonischen Beckensedimente im Rechtsrheinischen Schiefergebirge (Adorf Bänderschiefer). Cour Forsch Inst Senckenberg 163:1–153

Playford PE (1980) Devonian "Great Barrier Reef" of Canning Basin, Western Australia. Am Assoc Petrol Geol Bull 64:814–840

Rabien A (1956) Zur Stratigraphie und Fazies des Ober-Devons in der Waldecker Hauptmulde. Abh Hess LA Bodenforsch 16:1–83

Ribbert K-H, Skupin K, Oesterreich B (2006) Geologische Karte von Preussen und benachbarten Gebieten, von Nordrhein-Westfalen, 1:25000. Blatt Madfeld (4518)

Riding R (1991) Calcareous algae and stromatolites. Springer, Berlin Heidelberg New York

Salamon M, Königshof P (2010) Middle Devonian olistostromes in the Rheno-Hercynian (Rheinisches Schiefergebirge)—an indication of back arc rifting on the passive margin of Laurussia? Gondwana Res 17:281–291. doi:10.1016/j.gr.2009.10.004

Sepkoski JJ Jr (1995) Patterns of Phanerozoic extinctions: a perspective from global data bases. In: Walliser OH (ed) Global events and event stratigraphy. Springer, Berlin Heidelberg New York, pp 35–51

Städter T, Koch R (1987) Mikrofazielle und diagenetische Entwicklung einer devonischen Karbonatfolge (Givet) am SW-Rand des Briloner Sattels. Facies 17:215–229

Stow DAV, Piper DJW (1984) Fine-grained sediments: deep water processes and facies. Geol Soc Lond Spec Publ 15:1–659

Stritzke R (1990) Die Karbonatsedimentation im Briloner Vorriffbereich. Geol Jb D 95:253–315

Sunkel G (1990) Devonischer submariner Vulkanismus im Ostsauerland (Rheinisches Schiefergebirge): Vulkanaufbau, Magmenzusammensetzung und Alteration. Bochumer geol geotechn Arb 34:1–250

Tucker ME (1973) Sedimentology and diagenesis of Devonian pelagic limestones (Cephalopodenkalk) and associated sediments of the Rhenohercynian Geosyncline, West Germany. N Jb Geol Paläont Abh 142:320–350

Tucker ME (1974) Sedimentology of Palaeozoic pelagic limestones: the Devonian Griotte (Southern France) and Cephalopodenkalk (Germany). Spec Publ Int Assoc Sediment 1:71–92

Tucker ME, Wright VP (1990) Carbonate sedimentology. Blackwell, London

von Dechen H (1858) Geologische Karte der Rheinprovinz und der Provinz Westfalen 1: 80.000. (Hrsg.) Kgl Minist Handel Gewerbe öff Arbeit, Sect 18, Berleburg, Berlin

Warnke K (1997) Microbial carbonate production in a starved basin: the crenistria Limestone of the upper Viséan German Kulm facies. Palaeogeogr Palaeoclimatol Palaeoecol 130:209–225

Wehrmann A, Blieck A, Brocke R, Hertweck G, Jansen U, Königshof P, Plodowski G, Schindler E, Schultka S, Wilde V (2005) Palaeoenvironment and palaeoecology of intertidal deposits in a

Lower Devonian siliciclastic sequence of the Mosel Region, Germany. Palaios 20:101–120

Wendt J, Aigner T (1985) Facies patterns and depositional environments of Palaeozoic cephalopod limestones. Sediment Geol 44:263–300

Wendt J, Belka Z (1991) Age and depositional environment of Upper Devonian (early Frasnian to early Famennian) black shales and limestones (Kellwasser facies) in the eastern Anti-Atlas, Morocco. Facies 25:51–89

Ziegler AP (1982) Geological atlas of western and central Europe. Shell, Den Haag